Thermal Degradation and Crystallization Behavior of Blend-Based Nanocomposites: Role of Clay Network Formation

Javad Seyfi,[1] Iman Hejazi,[2] Gity Mir Mohamad Sadeghi,[2,3] Seyed Mohammad Davachi,[1] Sadegh Ghanbar[2]

[1]*Polymer Engineering and Color Technology Department, Amirkabir University of Technology, Tehran, Iran*
[2]*Department of Polymer Engineering, Amirkabir University of Technology, Tehran, Iran*
[3]*New Technologies Research Center, Amirkabir University of Technology, Tehran, Iran*

Received 19 August 2010; accepted 30 April 2011
DOI 10.1002/app.34814
Published online 24 August 2011 in Wiley Online Library (wileyonlinelibrary.com).

ABSTRACT: The main goal of this study is to explicate the exact role of nanoclay particles on thermal degradation mechanism and crystallization behavior of blend-based nanocomposites. Thermoplastic olefin (TPO) nanocomposites, as a simple model, were prepared via melt mixing in an internal batch mixer. X-ray diffractometry (XRD) and transmission electron microscopy tests show that a relatively good dispersion of silicate layers was obtained in the system. On the addition of nanoclay, a remarkable reduction in rubber domain size was observed through scanning electron microscopy (SEM). Thermogravimetric analysis shows that nanoclay particles can retard thermal decomposition process. Thermal degradation kinetic studies, using Flynn–Wall–Ozawa method, reveal that addition of nanoclay contents higher than 1 wt % changes the mechanism of thermal degradation. A mechanism was proposed to explain this phenomenon based on SEM images of char residues. Non-isothermal crystallization behavior of samples was investigated using differential scanning calorimeter. The unexpected reduction in crystallinity of TPO nanocomposites containing 5 wt % nanoclay was explained using rheometry analysis and attributed to the formation of stable percolated clay networks in this sample. © 2011 Wiley Periodicals, Inc. J Appl Polym Sci 123: 2492–2499, 2012

Key words: clay; degradation; kinetics; nanocomposites

INTRODUCTION

Thermoplastic elastomer materials based on polypropylene (PP) and ethylene propylene diene monomer (EPDM), often referred as thermoplastic olefins (TPOs), have gained special attention because of their excellent weatherability, low density, and relatively low cost. TPO materials have found wide applications in automotive parts, cable insulation, extruded profile for windows, footwear, packaging industry, etc.[1]

Within the fascinating world of nanomaterials in general, polymer–clay nanocomposites more than carry their weight in terms of intrigue and applicability. Consider all the factors that must be involved in the dramatic modification and improvement of a polymer's behavior on the addition of just a few weight percent (wt %) of a nano-size inorganic sheet compound.[2] Many studies have been devoted to investigate TPO/clay nanocomposites.[1,3–8] In our earlier study,[3] rheological and mechanical properties of these systems were investigated with the aim of determining the optimum nanoclay content and processing parameters. Lee et al.[5] reported that the aspect ratio of nanoclay particles and the apparent size of rubber phase decreased with increasing nanoclay content. They also attributed the improvement in mechanical properties to the morphological changes induced by the presence of nanoclay particles. Kim et al.[6] investigated the effect of compatibilizer/nanoclay ratio on morphology and mechanical properties of TPO nanocomposites and concluded that the ratio of Maleic anhydride-*grafted*-polypropylene (PP-g-MA)/nanoclay to obtain the desired balance of properties should be fixed at 1 : 1.

Non-isothermal crystallization study of polymers is more meaningful than isothermal crystallization study, because it is similar to conventional industrial processing. The effect of nanoclay content on non-isothermal crystallization behavior of TPO nanocomposites has been rarely studied. Frounchi et al.[8] reported that crystallinity of nanocomposites was relatively lower than the TPO blend suggesting that nanoclay inhibits the growth of spherulites of PP.

Thermal degradation of polymers is a very important phenomenon, which affects the performance of all polymeric materials in daily life.[9] The kinetic

Correspondence to: G. M. Mohamad Sadeghi (gsadeghi@aut.ac.ir).

analysis provides information on energy barriers of the degradation process and is used to explain the mechanism of degradation. Degradation kinetic parameters can be obtained from dynamic experiments by means of different methods.[10–13] To the best of our knowledge, analysis of the kinetics of the decomposition process of TPO blends in presence of nanoclay particles has not been reported. Thus, the aim of this work is to investigate the influence of nanoclay loading on the kinetics of thermal degradation of TPO blends using Flynn–Wall–Ozawa method. This study is also devoted to the investigation on the effects of variation in nanoclay content on morphology and nonisothermal crystallization behavior of TPO nanocomposites.

EXPERIMENTAL

Materials

The materials used in this work were commercial grades. PP (SEETEC H5300, density = 0.9 g/cm^3) was obtained from LG corporation with melt flow rate of 3.5 g/10min which was measured under a load of total mass of 2.16 kg at a temperature of 230°C. EPDM (vistalon 7500, density = 0.9 g/cm^3, 55% ethylene content) with Mooney viscosity of 82 ± 5 (at temperature of 125°C) was provided by Exxon Mobil (Baton Rouge, Louisiana). PP-g-MA (polybond 3200, MA content = 1.0 wt %) was supplied by Dupont and an organically modified montmorillonite (Cloisite 20A) was purchased from Southern Clay Products are used for preparing nanocomposites.

Sample preparation

All of the materials were dried at 80°C for 12 h before processing. The melt blending of the samples was conducted in a Brabender internal mixer (Germany) at 190°C, mixing time of 10 min and rotor speed of 60 rpm. Weight ratio of PP/EPDM blend was kept constant at 80/20 (w/w). A range of PP/EPDM nanocomposites containing 1, 3, 5, and 7 wt % nanoclay were also prepared (TPO1, TPO3, TPO5, and TPO7). For all nanocomposite samples, the PP-g-MA/nanoclay ratio was fixed constant at 1 : 1.

Characterization

Wide angle X-ray scattering analysis was carried out by an X-ray diffractometry (XRD; Xpert, Philips) operating at 40 kV and 30 mA for Cu K_α radiation (λ = 0.154 nm). The scanning rate was 1°/min with a step size of 0.04° under the diffraction angle, 2θ, in the range of 1–10°. Dispersion of nanoclay particles in the TPO matrix was examined by a Philips EM208S transmission electron microscope (TEM) with an accelerating voltage of 100 kV. Ultra thin sections of 70 nm thickness were cryogenically cut with a diamond knife at a temperature of −100°C. The morphologies of the blend and nanocomposite samples were analyzed using a Philips XL30 scanning electron microscope (SEM) with 16 kV accelerating voltage. The samples were kept in liquid nitrogen and then brittle fractured. The fracture surfaces were etched with toluene for 3 h at room temperature to dissolve out EPDM phase. A SCDOOS sputter coater was employed to coat the fracture surfaces with gold for increased conductivity. Morphological studies on the char residue after thermogravimetry analysis (TGA) were also performed. Non-isothermal crystallization of the TPO blend and nanocomposites was performed on an Elmer Diamond Differential Scanning Calorimeter (DSC). To investigate the non-isothermal crystallization behavior, all samples were first heated to 200°C at 10°C/min (heating scan), held at 200°C for 3 min to remove any thermal history, and then cooled to 55°C at 10°C/min (cooling scan). Crystallization peak temperatures were obtained from the cooling scan. Thermal stability of PP/EPDM blend and nanocomposites was investigated by non-isothermal TGA using a Perkin Elmer-Pyris1 TGA instrument. The measurements were conducted from 50 to 600°C at heating rates of 5, 10, and 20°C min^{-1} in a dynamic nitrogen atmosphere (flow rate of 50 mL min^{-1}). Rheological measurements were performed using a rotational rheometer (MCR 301, Physica, Germany) to measure the dynamic viscoelastic properties of the samples. Disk type parallel plates (gap of 0.5 mm and diameter of 25 mm) were employed, and all measurements were performed at 210°C. The dynamic moduli were measured in the angular frequency ranging from 0.05 to 500 s^{-1}, assuring the linear viscoelastic condition for dynamic measurement (γ = 0.2%) which was verified via an amplitude sweep test.

RESULTS AND DISCUSSION

Structure and morphology of TPO nanocomposites

Because PP is a non-polar thermoplastic, it is well-known that presence of a compatibilizer with polar groups, such as PP-g-MA, is a necessary prerequisite to achieve good dispersion of nanoclay particles in the TPO matrix.[6,14] Figure 1 presents XRD patterns of the nanoclay and various nanocomposites. The mean interlayer spacing of the (001) plane, $d_{(001)}$, for the pure Cloisite 20A powder obtained by XRD measurement is 24.5 Å. As shown in Figure 1, the (001) plane peaks of nanocomposites shift to the lower angles when compared with the neat nanoclay, which is reflective of an increase in the gallery

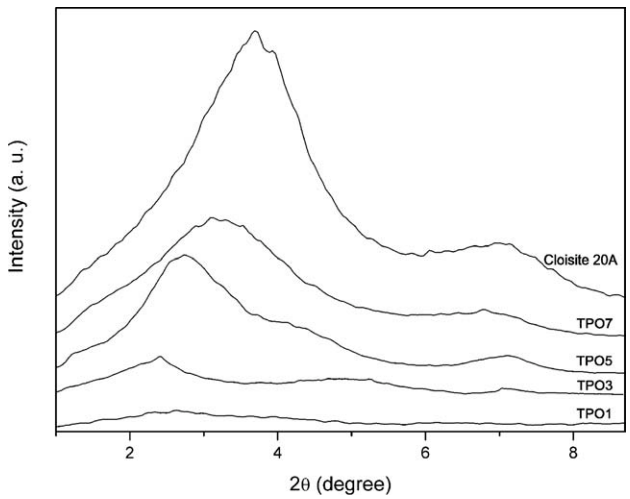

Figure 1 XRD spectra of nanoclay and TPO nanocomposites at various amounts of nanoclay loading.

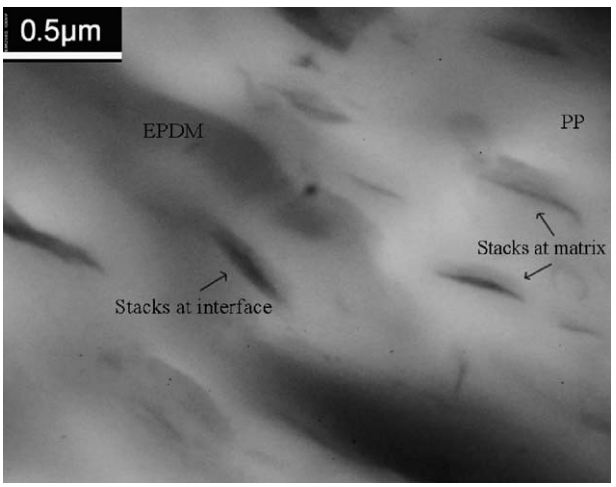

Figure 2 TEM image of TPO nanocomposite containing 3 wt.% nanoclay.

height of the silicate layers. Mehta et al.[7] showed that the clay platelets are largely located at the PP/EPDM interface, thus the increased d-spacing values indicate that polymer chains, mostly residing at the interface, intercalate into the galleries of nanoclay layers, which is confirmed by TEM results. In case of TPO1, a very small broad peak is observed which indicates that a very good dispersion of silicate layers occurred in the system. This peak appears with more intensity for TPO3, TPO5, and TPO7 suggesting that these nanocomposites have a mixed morphological structure, i.e., combination of tactoids and exfoliated silicate layers. This relatively good dispersion of clay layers in TPO matrix originates from the polar character of the anhydride which causes an affinity for the silicate surfaces, so that the maleated PP can act as a compatibilizer between the matrix and nanoclay.[6] Another reason for this relatively good dispersion could be high mobility of EPDM component, due to its high molecular weight and flexible chains which can easily move into the interlayer spaces of silicates during the melt blending process.[15] The observed shift for TPO3 and TPO5 to higher angles compared with TPO3 indicates lower interlayer distance between the silicate layers. The reason for this behavior could be partial degradation of organo-modifier molecules within the silicate layers during melt mixing.[16]

TPO nanocomposites containing 3 wt % nanoclay were further characterized by TEM and shown in Figure 2. The intercalation/exfoliation coexistence in TPO3 can be further verified via this figure; however, the majority of silicate layers are intercalated and only few ones are in the exfoliated state. It should be noticed that the dark thin lines represent nanoclay layers which are relatively well dispersed. It can be observed that clay stacks are largely located at the PP matrix and the PP/EPDM interface. The localization of clay layers at the interface of PP/EPDM blends was previously reported.[7]

The morphology of neat TPO blend and nanocomposite containing 3 wt % nanoclay is compared with SEM images and depicted in Figure 3. In these images, the black holes represent EPDM particles which have been dissolved out by toluene.

Figure 3(a) displays SEM image of the surface of neat TPO blend showing the dispersion of EPDM particles, which appear to be globular, in the PP

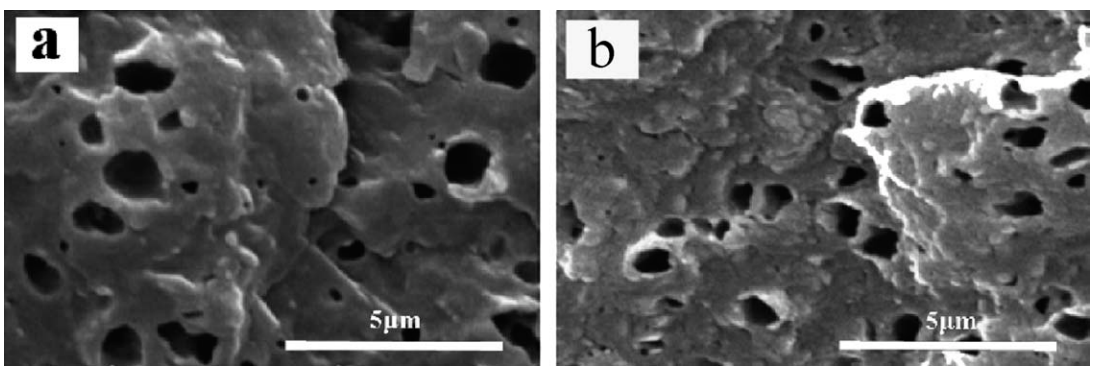

Figure 3 Cryogenic fractured and etched surfaces of the samples: (a) TPO and (b) TPO3.

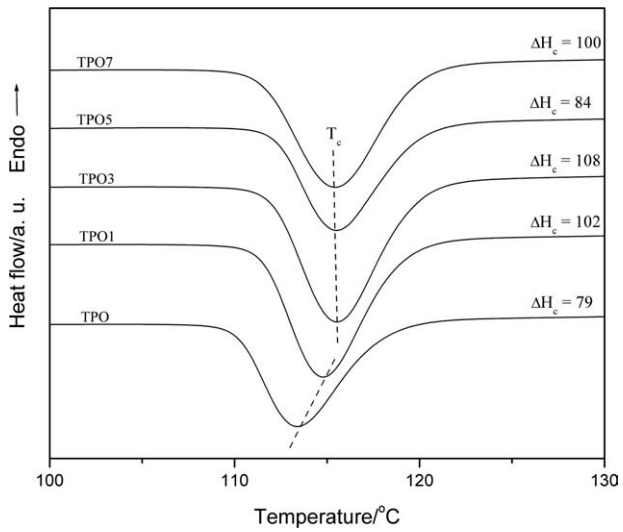

Figure 4 The crystallization exotherms of neat TPO blend and nanocomposites with different amounts of nanoclay loading for non-isothermal crystallization from the melt at a cooling rate of 10°C/min.

matrix. The incorporation of 3 wt % nanoclay into the TPO blend leads to a reduction in the size of the dispersed EPDM phase. Another observation is that addition of the nanoclay content results in more elongated shape than that of neat TPO blend, as shown in Figure 3. Similar behavior has been reported by several authors.[4–7] Variations in the morphology of the EPDM phase with addition of nanoclay content, e.g., decrease in size and increase in irregularity of particle shape, may originate from two compounding effects during melt-processing; one is increasing of melt viscosity due to the presence of clay particles which might control the particle size of rubbery phase via shear-mixing coalescence and breakup.[7] One could state that rigid clay particles increase the melt viscosity of the matrix phase which could prevent the coalescence of dispersed phase particles because of the reduced mobility of polymer chains in the system. Although, second is the intercalation of silicate layers which could suppress the coalescence and agglomeration of the rubbery phase particles. Khatua et al.[17] demonstrated that clay particles caused a reduction in the size and stability of dispersed elastomer domains in a nylon 6 matrix via this barrier effect to coalescence mechanism.

Crystallization behavior

To investigate the effect of various nanoclay loadings on crystallization behavior of PP/EPDM blends, DSC measurements were carried out. Because most processing methods occur under non-isothermal conditions, the understanding of polymer crystallization under dynamic conditions is of considerable importance.[18] The crystallization exotherms of the TPO blend and nanocomposites are presented in Figure 4. The characteristic parameters of non-isothermal crystallization exotherms such as the crystallization peak temperature (T_c), the relative degree of crystallinity (X_t), in terms of ΔH_c (H_c is the enthalpy of crystallization), and width at half height of crystallization peaks (WHH) are reported in Table I.

It can be observed that with the incorporation of nanoclay into the blend, the crystallization peaks shift to higher temperatures, albeit not significantly. Such behavior was reported numerously in the literature.[18–21] It is also clear from Table I that the crystallization peaks are narrower on addition of nanoclay loading up to 5 wt %. Higher crystallization temperatures and narrower peak widths indicate an increased crystallization rate in the nanocomposites. This phenomenon has been reported in nanocomposites based on semicrystalline polymers which was attributed to the absorption of polymer chains by nanoclay layers and nucleating role of nanoclay particles.[20] However, the width of crystallization peak increases for TPO7 which indicates the slower rate of nucleation, and therefore, wider crystallite size distribution. A closer scrutiny on the data reported in Table I reveals that, below 3 wt % nanoclay content, crystallization temperature (T_c) increases with the content of nanoclay; but above 3 wt %, T_c shows no further enhancement and decreases slightly with increasing concentration of nanoclay. It also can be seen that the same trend appeared for the relative degree of crystallinity (X_t) of nanocomposites, that is, with the addition of nanoclay content to 3 wt %, X_t enhanced by nearly 37%. This phenomenon can be explained by the fact that presence of nanoclay platelets in the TPO matrix promotes heterogeneous nucleation which leads to an increase in the crystallization rate and the degree of crystallinity of nanocomposites. Above 3 wt % nanoclay, the crystallinity of PP component in TPO matrix diminishes. This may be due to the fact that at high amounts of nanoclay content in the TPO matrix, silicate layers, either in form of tactoids or platelets, can act as obstacles for mobility and flexibility of the PP chains to fold and join the crystallization growth front, and finally lead to a reduction in ΔH_c values.[18] However, in case of TPO nanocomposites, with increasing nanoclay loading from 5 to 7 wt %,

TABLE I
T_c, ΔH_c, and Width at Half Height of Crystallization Peak (WHH) of TPO Blend and Nanocomposites

Samples	TPO	TPO1	TPO3	TPO5	TPO7
T_c (°C)	113.3	114.8	115.6	115.5	115.4
ΔH_c (J/g)	79	102	108	84	100
WHH (°C)	4.83	4.60	4.75	4.71	5.12

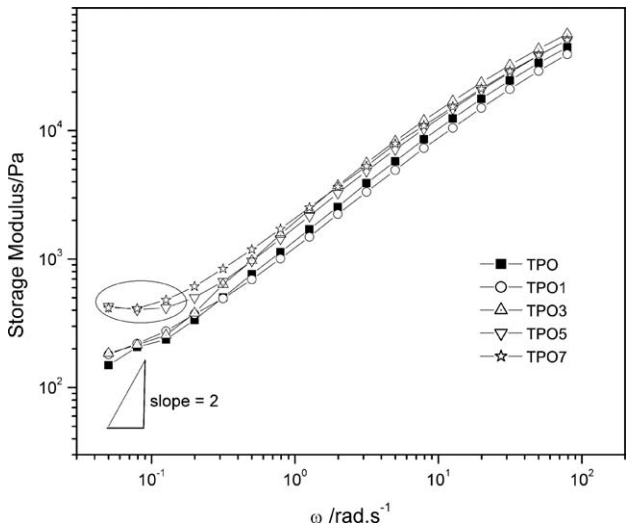

Figure 5 Frequency dependence of the storage modulus, G', of TPO blend and nanocomposites at 210°C.

not only the crystallinity degree did not diminish but also enhanced by nearly 19%.

To explain this unexpected behavior, rheology of the system was analyzed. Storage modulus, $G'(\omega)$, of TPO blend and nanocomposites containing different amounts of nanoclay loading are shown in Figure 5. It is well-established that the rheological response of pure polymers is typical of an entangled polymer melt (slope of $G'(\omega) = 2$), whereas the nanocomposites show pseudo-solid-like behavior.[21] As can be seen in Figure 5, in case of the neat TPO, slope of G' is significantly decreased at low frequencies which can be very probably attributed to the incorporation of a rubbery material (EPDM) into PP matrix. The reduction in frequency dependence of G' is most pronounced at high loadings of nanoclay content (5 and 7 wt %), in which a plateau is observed at low frequencies. This pseudo-solid-like response stems from large frictional interaction of the silicate layers which are randomly oriented and form a percolated network structure incapable of relaxing completely.[22] Another noticeable point, which is marked in the figure, is that TPO5 shows a weaker frequency dependence of G' when compared with TPO7 indicating the formation of a more stable three-dimensional percolated network. Hence, it is reasonable to claim that the more stable the percolated network, the less mobile and flexible the polymer chains become. This can be explained by the fact that the highly restrictive environment around these networks may hinder the relaxation of PP chains in the TPO matrix causing a reduction in their mobility which could restrain the growth of crystallites and finally diminish the crystallinity in TPO5 when compared with TPO7. This could be the reason for the unexpected reduction in crystallinity of TPO5 relative to other samples with different amounts of nanoclay content.

Thermal degradation of TPO blend and nanocomposites

Thermal stability of the neat TPO blend and nanocomposites was measured by TGA in nitrogen atmosphere at three different heating rates. Figure 6 presents the typical TGA traces of weight loss as a function of temperature of the neat TPO blend and nanocomposites in pyrolytic environment at heating rate of 10°C/min.

It is generally known that the addition of nanoclay particles into polymers could improve their thermal stabilities.[23] On one hand, this improvement can be attributed to the formation of a protective barrier of ablative silicate layers on the remaining polymer. On the other hand, it can be related to the torturous path for volatile products whereby volatilization might be delayed. The shape of TGA curves in Figure 6 shows that in earlier stages of thermal decomposition, the degradation process is retarded to higher temperatures by addition of nanoclay into the blend. Dispersed silicate layers in the TPO matrix, either in shape of tactoids or exfoliated platelets, may act as heat insulator and mass transport barrier and improve the thermal stability of the blends up to temperatures above 400°C.[24] However, the weight loss curves of nanocomposites containing 3, 5, and 7 wt % were almost vertical indicating a very rapid decomposition process. The reason may arise from the fact that in these samples, stacked silicate layers could hold accumulated heat that can be used as a heat source to accelerate the degradation process.[25] Another possible reason for this

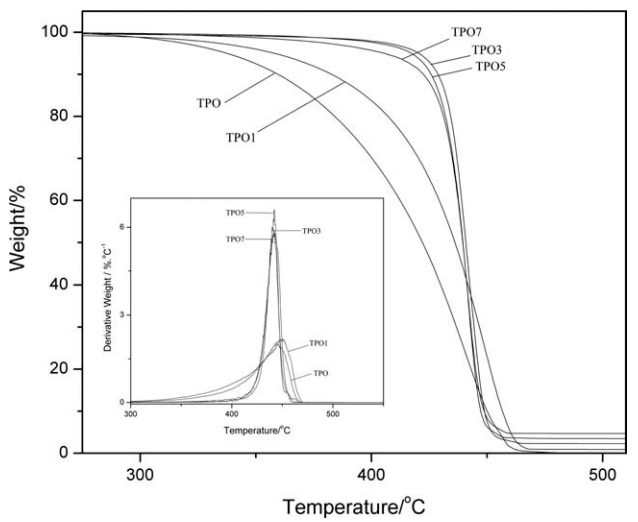

Figure 6 TGA thermograms of the neat TPO blend and nanocomposites at a heating rate of 10°C/min in N_2 atmosphere. Inset shows DTGA curves.

TABLE II
The Characteristics of the TGA Curves for TPO Blend and Nanocomposites

Nanoclay (%)	0	1	3	5	7
T_{onset} (°C) (±3)	337	358	420	417	405
T_{max} (°C) (±1)	445	449	442	442	441.5
% Char (±0.4)	0	0.84	2.25	3.54	4.64

observation could be the degradation of organic modifiers within the Cloisite 20A layers, which was reported in range of 300–500°C.[26] It is known that degradation of organic molecules used in nanoclay leads to the creation of active catalytic sites in the polymer matrix[27,28] which could accelerate the decomposition of the whole system. The vertical shape of TGA curves can also be attributed to the fact that at high temperatures (above 400°C), degradation of the clay network which covers the surface of the remaining polymer leads to formation of some holes in it. Therefore, faster migration of degradation products and bubbles from the remaining mass occurs which results in a very fast weight loss in the system. The role of the clay network on thermal degradation mechanism of TPO nanocomposites will be further discussed in the next section.

The characteristics of the TGA curves for all the samples are listed in Table II. The onset temperature of degradation, the temperature corresponding to 5% weight loss, is increased from 337 to 358°C via addition of only 1 wt % nanoclay into the blend. As shown in Table II, the most profound enhancement in T_{onset} of degradation (83°C) is observed in case of adding 3 wt % nanoclay. It is interesting to note that with increasing nanoclay content from 3 to 5 and 7 wt %, thermal stability of the system was no further improved. Such behavior could be attributed to the relative extent of exfoliation.[10] Because at high nanoclay contents, according to XRD results, exfoliation of silicate layers becomes more hindered due to geometrical constraints within the polymer matrix, thus no more significant increase in thermal stability is expected. DTG curves of the samples in nitrogen at heating rate of 10°C are also shown in Figure 6 as inset. As can be observed from DTG curves, the temperature range, in which thermal degradation occurs, is noticeably reduced for nanocomposites containing higher nanoclay loadings than 1 wt %.

Table II also reports the amounts of char residues of all the samples. As is clear, increasing the nanoclay content causes an enhancement in formation of carbonaceous char leading to higher percentage of char residues. Formation of such a carbonaceous–silicate char on the surface during the pyrolysis could insulate the underlying material leading to slower mass loss rate of degradation products.[29]

Kinetics of thermal degradation

To better understand the degradation mechanism, a kinetic analysis may be performed. Thus, activation energies of degradation were calculated using FWO method as a function of degree of conversion. This model describes a rather simple method of calculating activation energy directly from weight loss versus temperature data obtained at several heating rates, using the equation[30,31]:

$$\log \varphi = \log \frac{AE_\alpha}{g(\alpha)R} - 2.315 - \frac{0.4567E_\alpha}{RT} \qquad (1)$$

where φ is the heating rate, A is the pre-exponential factor, E_a is the activation energy of degradation, $g(\alpha)$ is the integral function of conversion, R is the gas constant, and T is the absolute temperature. The activation energy for different conversion values can be calculated from plots of log φ versus $1/T$ which are shown in Figure 7. Thus, values of α between 0.1 and 0.9 and φ values of 5, 10, and 20°C/min were selected to obtain the activation energies as a function of conversion, which are shown in Figure 8 for the neat TPO blend and nanocomposites. It is clear that introduction of 1 wt % nanoclay into the neat TPO increases the activation energy values, and thus, thermal stability of the neat blend. This increase in activation energies is in conformity with the experimental data shown in TGA graphs (Fig. 6). It is generally believed that the addition of nanofillers into the polymers can improve their thermal stabilities which can be attributed to the shielding effect of nanoclay layers.[23] By taking a glance at Figure 8, one could see that activation energy values for the neat TPO and TPO1 increase monotonously with the degree of conversion, whereas for TPO3,

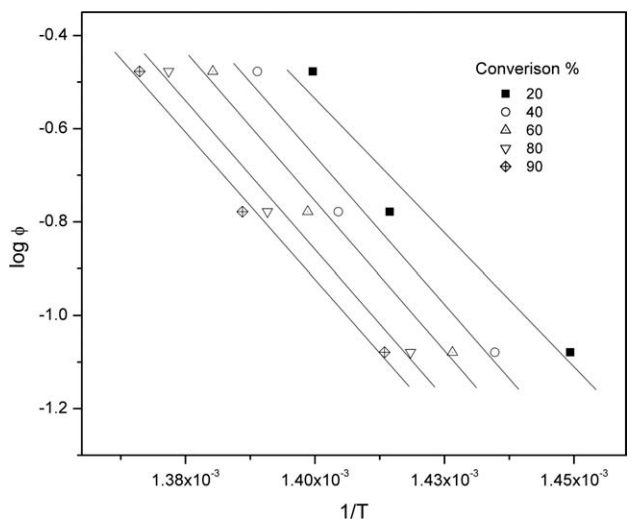

Figure 7 Determination of the degradation activation energy for TPO3.

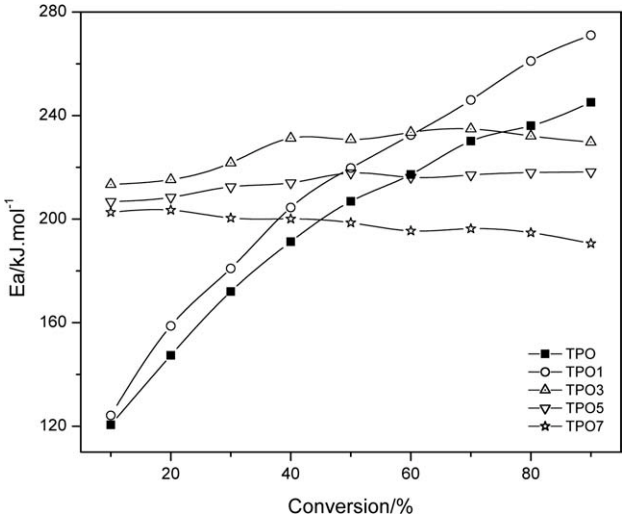

Figure 8 Activation energy as a function of conversion for TPO blend and nanocomposites.

TPO5, and TPO7 are nearly constant. The variation in E_a values for TPO and TPO1 might be due to changes in reaction mechanism during decomposition process. The same behavior was also reported in the literature.[32–34] On the basis of these reports, this variation can be attributed to the nature of random chain scission degradation which is independent of the heating rate. It is important to note that the degradation temperature could affect the size of volatile products. With increasing temperature, the minimum size of volatile particles increases, thus, the rate of weight loss is related to both of scission rate of polymer chains and size of volatile products. Therefore, the dependence of size distribution of volatile products on heating rate and the random chain scission nature of degradation mechanism of PP could be major reasons for the ascending trend of activation energy values of the aforementioned samples.[33,35]

Another interesting observation is that addition of higher nanoclay contents leads to a change in shape of activation energy plots. Nanocomposites containing 3, 5, and 7 wt % seem to have a different decomposition trend implying the influence of nanoclay content on the degradation mechanism. We believe that the change in trend of E_a values could be ascribed to the impact of nanoclay networks on the size distribution of volatile products. Because the boiling temperatures of most of degradation products are lower than the thermal degradation temperatures of polymers, bubbles can nucleate below the surface of the remaining polymer and gradually transform into the gas phase.[36] It has been reported that nanofillers such as nanoclay particles can reduce the flammability of polymers by inhibiting this vigorous bubbling process in the course of degradation during pyrolysis.[36–38] Therefore, in case of TPO nanocomposites containing higher than 1 wt % nanoclay, it is reasonable to deduce that the accumulation of clay particles on the sample surface hinders the migration of volatile products from the remaining mass, and thus, only very small particles can be released from the polymer residue leading to a narrower size distribution of volatile products. This might be the reason for disappearing the inconstancy in E_a values observed in case of neat TPO and TPO1. The accumulation of clay particles on the surface of the remaining polymer is shown in SEM images of the char residues of TPO3 and TPO5 samples in Figure 9. These figures clearly show the formation of an extended island-like structure made of clay and carbonaceous char during the pyrolytic decomposition[36] and further confirmed the above hypothesis.

As can be seen in Figure 8, TPO3 shows the highest activation energies until 60% conversion is reached. After that, quite unexpectedly, the sample containing 1 wt % nanoclay (TPO1) shows higher E_a values. Moreover, E_a values of TPO3 become even smaller than those of neat TPO just after 80% conversion. As mentioned earlier, this phenomenon could be explained by formation of some holes in the network of carbonaceous/silicate char, covering

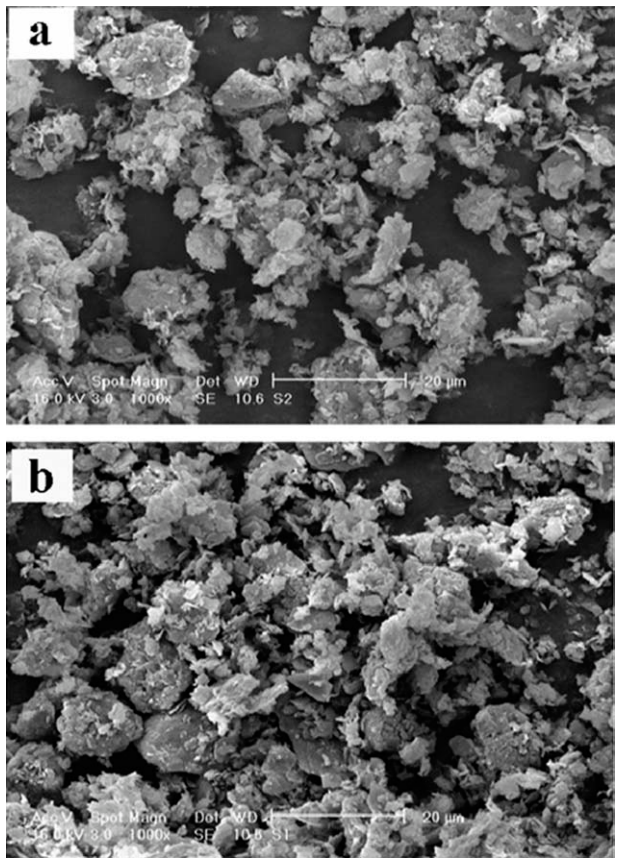

Figure 9 SEM micrographs of char residues from (a) TPO3 and (b) TPO5 samples after TGA experiments.

the remaining polymeric mass, at higher conversions leading to a very rapid evacuation of degradation products trapped inside the polymeric mass. This causes the activation energies of nanocomposites with higher than 1 wt % nanoclay not to increase at the final stages of decomposition process leading to lower Ea values when compared with the nanocomposite with 1 wt % nanoclay.

CONCLUSIONS

A melt mixing method was employed to prepare PP/EPDM blend and nanocomposites. XRD and TEM results showed that a relatively good dispersion of clay layers in TPO matrix was obtained which attributed to the high compatibility of polar PP-g-MA chains and organo-modified silicate layers. On the basis of SEM analysis, addition of compatibilizer and nanoclay into the blend reduced the size of EPDM dispersed phase. DSC results revealed that, below 3 wt % nanoclay content, crystallization temperature (T_c), and degree of crystallinity (X_t) increase with the content of nanoclay which is due to the nucleating role of nanoclay particles; but above 3 wt %, T_c and X_t show no further enhancement and decrease slightly with increasing concentration of nanoclay. The unexpected reduction in crystallinity of TPO5 was attributed to the formation of a more stable percolated clay network in case of adding 5 wt % nanoclay. Thermal degradation of TPO blend and nanocomposites was studied and fully described using a kinetic analysis by FWO method. The highest onset temperature of degradation was observed in nanocomposites containing 3 wt % nanoclay. It was found that addition of higher than 1 wt % nanoclay leads to a change in trend of E_a with degree of conversion. We proposed that this phenomenon can be attributed to the role of clay networks which could cover the surface of the remaining mass and hinder the migration of volatile products during the decomposition process. The accumulated clay particles and their island-like structures were shown using SEM images of the char residues.

Partial financial support from the Iranian Nanotechnology Initiative is gratefully appreciated.

References

1. Mishra, J. K.; Hwang, K. J.; Ha, C. S. Polymer 2005, 46, 1995.
2. Shonaike, G. O. Advanced Polymeric Materials; CRC Press: New York, 2003.
3. Hejazi, I.; Seyfi, J.; Sadeghi, G. M. M.; Davachi, S. M. Mater Des 2011, 32, 649.
4. Lee, H. S.; Fasulo, P. D.; Rodgers, W. R.; Paul, D. R. Polymer 2006, 47, 3528.
5. Lee, H. S.; Fasulo, P. D.; Rodgers, W. R.; Paul, D. R. Polymer 2005, 46, 1673.
6. Kim, D. H.; Fasulo, P. D.; Rodgers, W. R.; Paul, D. R. Polymer 2007, 48, 5960.
7. Mehta, S.; Mirabella, F. M.; Rufener, K.; Bafna, A. J App Polym Sci 2004, 92, 928.
8. Frounchi, M.; Dadbin, S.; Salehpour, Z.; Noferesti, M. J Mem Sci 2006, 142, 282.
9. Kumar, A. P.; Depan, D.; Tomer, N. S.; Singh, R. P. Prog Polym Sci 2009, 34, 479.
10. Chen, G. X.; Yoon, J. S. Polym Degrad Stab 2005, 88, 206.
11. Zong, R.; Hu, Y.; Wang, S.; Song, L. Polym Degrad Stab 2004, 83, 423.
12. Zhang, Y.; Xia, Z.; Huang, H.; Chen, H. Polym Test 2009, 28, 264.
13. Yang, M. H.; Tsay, D. K.; Wang, J. H. Polym Test 2002, 21, 737.
14. Wang, Y.; Chen, F. B.; Li, Y. C.; Wu, K. C. Composites B 2004, 35, 111.
15. Ma, J.; Xu, J.; Ren, J. H.; Yu, Z. Z.; Mai, Y. W. Polymer 2003, 44, 4619.
16. Shah, K. R.; Paul, D. R. Polymer 2004, 45, 299.
17. Khatua, B. B.; Lee, D. J.; Kim, H. Y.; Kim, J. K. Macromolecules 2004, 37, 2454.
18. Ray, S. S.; Bandyopadhyay, J.; Bousmina, M. Macromol Mater Eng 2007, 292, 729.
19. Wu, Z.; Zhou, C.; Zhu, N. Polym Test 2002, 21, 479.
20. Xu, W. B.; Zhai, H. B.; Guo, H. Y.; Zhou, Z. F.; Whiteley, N.; Pan, W. P. J Therm Anal Cal 2004, 78, 101.
21. Galgali, G.; Ramesh, C.; Lele, A.; Macromolecules 2001, 34, 852.
22. Wang, Y.; Chen, F. B.; Wu, K. C.; Wang, J. C. Polym Eng Sci doi:10.1002/pen.20471.
23. Leszczynska, A.; Njuguna, J.; Pielichowski, K.; Banerjee, J. R. Thermochim Acta 2007, 454, 1.
24. Gilman, J. W. Appl Clay Sci 1999, 15, 31.
25. Zhou, Q.; Xanthos, M. Polym Degrad Stab 2009, 94, 327.
26. Cervantes-Uc, J. M.; Cauich-Rodriguez, J. V.; Vazquez-Torres, H.; Garfias-Mesias, L. F.; Paul, D. R. Thermochim Acta 2007, 457, 92.
27. Zanetti, M.; Camino, G.; Thomann, R.; Mulhaupt, R. Polymer 2001, 42, 4501.
28. Preston, C. M. L.; Amarasinghe, G.; Hopewell, J. L.; Shanks, R. A.; Mathys, Z. Polym Degrad Stab 2004, 84, 533.
29. Gilman, J. W.; Jackson, C. L.; Morgan, A. B.; Harris, R. Chem Mater 2000, 12, 1866.
30. Ozawa, T. Bull Chen Soc Jpn 1965, 38, 1881.
31. Flynn, J. H.; Wall, J. Res Natl Bur Stand 1966, 70A, 487.
32. Chan, J. H.; Balke, S. T. Polym Degrad Stab 1997, 57, 135.
33. Gao, Z.; Kaneko, T.; Amasaki, I.; Nakada, M. Polym Degrad Stab 2003, 80, 269.
34. Day, M.; Cooney, J. D.; MacKinnon, M. Polym Degrad Stab 1995, 48, 341.
35. Gao, Z.; Amasaki, I.; Nakada, M. J Anal Appl Pyrol 2003, 67, 1.
36. Kashiwagi, T.; Du, F.; Douglas, J. F.; Winey, K. I. Harris, R. H., Jr.; Shields, J. R. Nat Mater 2005, 4, 928.
37. Kashiwagi, T.; Harris, R. H., Jr.; Zhang, X.; Briber, R. M.; Cipriano, B. H.; Raghavan, S. R.; Awad, W. H.; Shields, J. R. Polymer 2004, 45, 881.
38. Kashiwagi, T.; Mu, M.; Winey, K.; Cipriano, B.; Raghavan, S. R.; Pack, S.; Rafailovich, M.; Yang, Y.; Grulke, E.; Shields, J.; Harris, R.; Douglas, J. Polymer 2008, 49, 4358.